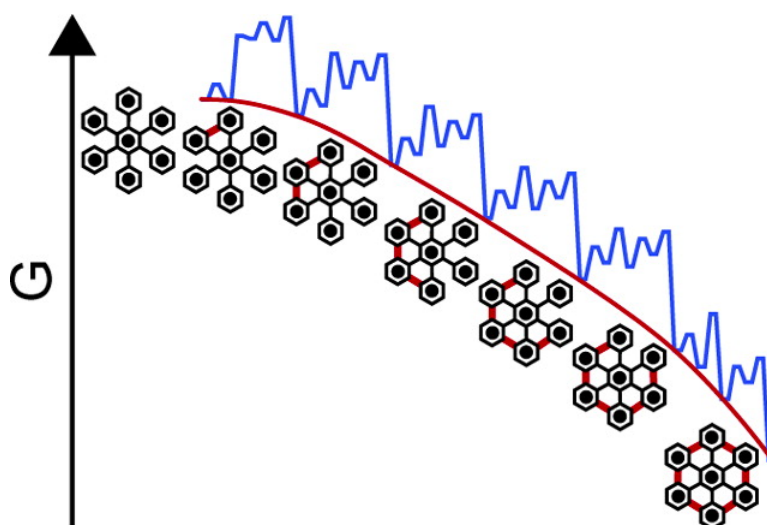


A Slippery Slope: Mechanistic Analysis of the Intramolecular Scholl Reaction of Hexaphenylbenzene

Pawel Rempala, Ji Kroulk, and Benjamin T. King

J. Am. Chem. Soc., **2004**, 126 (46), 15002-15003 • DOI: 10.1021/ja046513d • Publication Date (Web): 28 October 2004

Downloaded from <http://pubs.acs.org> on April 5, 2009



More About This Article

Additional resources and features associated with this article are available within the HTML version:

- Supporting Information
- Links to the 1 articles that cite this article, as of the time of this article download
- Access to high resolution figures
- Links to articles and content related to this article
- Copyright permission to reproduce figures and/or text from this article

[View the Full Text HTML](#)

A Slippery Slope: Mechanistic Analysis of the Intramolecular Scholl Reaction of Hexaphenylbenzene

Pawel Rempala, Jiří Kroulík, and Benjamin T. King*

Department of Chemistry, University of Nevada, Reno, Nevada 89557

Received June 12, 2004; E-mail: king@chem.unr.edu

The Scholl reaction¹ is the acid-catalyzed oxidative condensation of aryl groups. In a series of papers,^{2–4} Müllen and co-workers have demonstrated that the intramolecular variation is useful for the synthesis of large polycyclic aromatic hydrocarbons (PAHs) from dendritic arene precursors. Many C–C bonds between unfunctionalized aryl moieties can be formed; the current record is 126 bonds.⁴ The Scholl reaction also holds yet-unrealized promise for the synthesis of carbon nanotube segments⁵ and has been used to prepare hexaalkoxytriphenylenes from *o*-dialkoxybenzenes.⁶ The Kovacic conditions,⁷ which use transition metal salts such as MoCl₅, CuCl₂, or FeCl₃, are popular. Recently, it was reported that, in the course of the Scholl oxidation of hexaphenylbenzene (**1**), intermediate **2** was produced along with the expected product hexa-*peri*-benzocoronene (**3**) (Scheme 1).^{3,8} While the identification of **2** is important, little else is known about the mechanism of this reaction. Some related reactions, like the oxidative coupling of phenols, are satisfactorily explained by radical processes.⁹ Other related reactions, like the oxidative coupling of aryl- or alkoxy-substituted arenes, are proposed to occur via radical cations^{10,11} or arenium cations.¹¹

We present a computational¹² and experimental study on the mechanism of a prototypical intramolecular Scholl condensation, the conversion of **1** to **3** (Scheme 1).

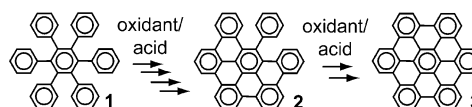
The *o*-terphenyl (**4**) model system (Scheme 2) was examined first to determine which of the proposed¹¹ mechanistic pathways, arenium or radical cation based, is most likely.

Since the exact nature of the proton transfer and the oxidative dehydrogenation transition states (TSs) is not obvious, these TSs were not calculated. Instead, literature values were adopted. For proton transfers, we used the average value of 4.0 kcal/mol calculated for the hydronium ion/benzene system.¹³ For the oxidations, we used the value of 6.8 kcal/mol measured for dehydrogenation of 9,10-dihydroanthracene by nitrobenzene.¹⁴

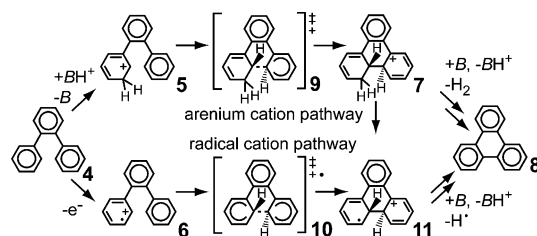
To compare the two reaction pathways, the same net energetic outcome is required. We chose protonated *o*-terphenyl (**5**) as the acid, which corresponds to a catalytic amount of a strong Brønsted acid in a weakly basic solvent. Hence, **4** → **5** is degenerate. Since the radical cation pathway requires two individual one-electron oxidations and the arenium cation pathway requires the single-step formal loss of H₂, the following schemes were applied: **4** + *O* → **6** + *R*; deprotonated **7** + 2*O* + 2*B* → **8** + 2*R* + 2 *B*·H⁺, where *O* is an one-electron oxidant, *R* is its reduced form, and *B* is the conjugate base, *o*-terphenyl. In addition, the first step, **4** + *O* → **6** + *R*, is set so Δ*G* = 0, which will require a strong oxidant, as **4** has high ionization potential (vacuum adiabatic, B3LYP/6-31G(d), 7.22 eV; B3LYP/6-311+G(d,p)//B3LYP/6-31G(d), 7.53 eV; photoelectron spectroscopy,¹⁵ 7.99 eV; this discrepancy is not unusual¹⁶).

The trans C–C bond-forming TSs **9** and **10** are significantly lower in energy than their cis counterparts. Both vacuum and solvated data suggest that the arenium cation pathway is preferred over the radical cation pathway (Figure 1).

Scheme 1. Hexaphenylbenzene Condensation



Scheme 2. Arenium Cation and Radical Cation *o*-Terphenyl Condensation Pathways



On the basis of the *o*-terphenyl results, the arenium cation-based mechanism was calculated for the conversion of **1** to **3**. Energies are based on protonated **1** (**1**·H⁺) as the acid and evolution of H₂. Each C–C bond-forming step is consummated, restoring aromatic stabilization, before the next begins. Aryl–aryl bonds are introduced along the pathway having the least strained fully benzenoid intermediates; this pathway happens to be contiguous. Since the Curtin–Hammett principle¹⁷ is likely to apply, C–C bond-forming TSs resulting from protonation at different sites were considered. Scheme 3 illustrates two paths from **12** to **13**. In the first, ortho protonation of a phenyl group results in arenium ion **14**. In the second, the more basic PAH core is protonated at the δ position, leading to **15**.

The *o*-phenyl and δ-PAH protonation pathways, which intersect at the fully aromatic points **a**₁ = **1**, **a**₂ = **12**, **a**₃ = **13**, **a**₄, **a**₅ = **2**, **a**₆, and **a**₇ = **3**, continue until fully condensed **3** is formed (Figure 2). The energies of the C–C bond-forming TSs in the δ-PAH series (**d**_{*i*}^δ) with respect to the most stable arenium ion (**c**_{*i*}^δ) decrease in the δ-PAH series, with the exception of the last step. The C–C bond-forming TS energies of the *o*-phenyl pathway (**d**_{*i*}^o) are greater than those of the δ-PAH pathway, indicating that the δ-PAH protonation pathway is preferred.

It is noteworthy that consecutive condensation steps are increasingly exergonic. Likewise, the energy of the dehydrogenation TSs **h**_{*i*} relative to **a**_{*i*} also decreases in this series. This is not unexpected, as it is estimated to lie 6.8 kcal/mol above the preceding dihydro compound **g**_{*i*}. The increasing exergonicity correlates reasonably with increasing resonance energy per π electron¹⁸ (REPE) of growing PAH core (3.43, 3.53, 3.55, 3.50, 3.63 kcal/mol for *i* = 2, 3, 4, 5, 6, 7, respectively; cf. benzene, 3.34 kcal/mol). Since the curve connecting points **a**_{*i*} is convex, the reaction contour resembles a slippery slope.

The Hammond postulate¹⁹ is manifest in this reaction. For both pathways, the nascent CC bond is shortest in the least exothermic first step (Table 1).

The identity of the rate-determining TS is determined by the strength of the catalytic acid. Stronger acids will stabilize the proto-

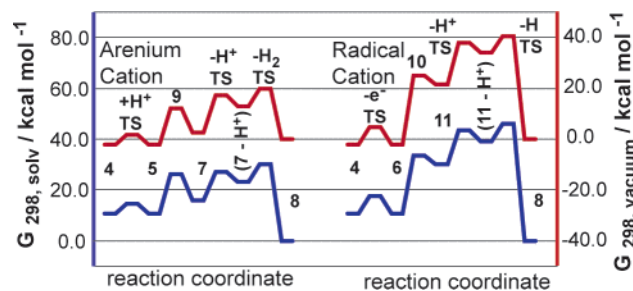


Figure 1. Free energy diagrams (red, vacuum; blue, solvated) for arenium cation and radical cation *o*-terphenyl condensation pathways.

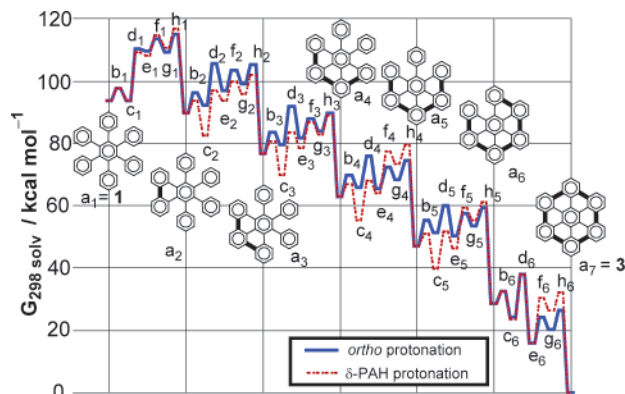


Figure 2. Reaction coordinate diagram for **1** \rightarrow **3**. Labels: **a**_{*i*} as shown; **b**_{*i*} protonation TS; **c**_{*i*} arenium cation; **d**_{*i*} C–C bond formation TS; **e**_{*i*} protonated dihydro intermediate; **f**_{*i*} deprotonation TS; **g**_{*i*} neutral dihydro intermediate; **h**_{*i*} oxidation TS.

Scheme 3. Hexaphenylbenzene Condensation

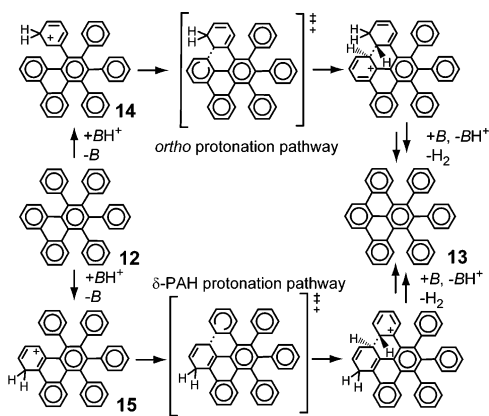


Table 1. Free Energies and TS CC Lengths (kcal/mol, Å)

step	$\Delta G_{298,\text{solv}}$	$\Delta G(\text{d}^{\text{p},\delta} - \text{c}^{\text{p}})_{298,\text{solv}}$		$R(\text{C}\cdots\text{C})\text{d}^{\text{p},\delta}$	
		<i>o</i> -Ph	δ -PAH	<i>o</i> -Ph	δ -PAH
1 (a ₁ \rightarrow a ₂)	−4.03	16.43	15.31	1.90	1.89
2 (a ₂ \rightarrow a ₃)	−13.06	22.98	14.64	2.04	1.93
3 (a ₃ \rightarrow a ₄)	−13.93	22.07	13.65	2.08	1.97
4 (a ₄ \rightarrow a ₅)	−15.76	20.52	12.64	2.11	1.95
5 (a ₅ \rightarrow a ₆)	−18.35	20.14	12.07	2.10	1.96
6 (a ₆ \rightarrow a ₇)	−28.66	14.59	14.71	2.05	2.09

nated stationary points **c**_{*i*}, **d**_{*i*}, and **e**_{*i*} relative to the unprotonated stationary points **g**_{*i*} and **h**_{*i*}. Conversely, weaker acids will stabilize the unprotonated stationary points **g**_{*i*} and **h**_{*i*} relative to the protonated stationary points **c**_{*i*}, **d**_{*i*}, and **e**_{*i*}. It follows that dehydrogenation will be rate determining in the stronger acids, and either C–C bond formation or proton transfer will be rate determining in the weaker acids.

In our laboratories, oxidation of hexaphenylbenzene with substoichiometric oxidant (CuCl_2 , $\text{PhI}(\text{O}_2\text{CCF}_3)_2$, FeCl_3 , or MoCl_5) affords only **3** and unreacted **1** with nearly quantitative mass balance. After separation of insoluble **3**, HPLC/diode array UV analysis of reaction mixtures revealed unreacted hexaphenylbenzene containing small quantities of compounds exhibiting a UV spectrum consistent with chlorinated **1**, or, in one instance, a small quantity of a compound exhibiting a UV spectrum consistent with a PAH. These experiments are consistent with the calculated arenium cation reaction profile.

The unexpectedly clean intramolecular hexacyclization of hexakis(chloroacetamido)benzene²⁰ also occurs without accumulation of intermediates. This reaction was investigated by analogous substoichiometric mass balance experiments.

In summary, the intramolecular Scholl reaction of hexaphenylbenzene likely proceeds by protonation, electrophilic attack, deprotonation, and subsequent oxidation. C–C bonds are likely formed stepwise and contiguously, with the first being formed the slowest. The reaction is increasingly exergonic, possible due to increasing REPE. It is likely that the utility of the Scholl reaction for the formation of large PAHs arises from the slippery slope phenomenon.

Acknowledgment. This work was supported by an award from the Research Corporation and by the University of Nevada. Acknowledgment is made to the Donors of the American Chemical Society Petroleum Research Fund for partial support of this research. We thank Prof. S. H. Gellman for alerting us to ref 20.

Supporting Information Available: Computational details, energies, coordinates, and experimental procedures. This material is available free of charge via the Internet at <http://pubs.acs.org>.

References

- Scholl, R.; Mansfeld, J. *Ber. Dtsch. Chem. Ges.* **1910**, *43*, 1734–1746.
- Fechtenkötter, A.; Tchebotareva, N.; Watson, M.; Müllen, K. *Tetrahedron* **2001**, *57*, 3769–3783. Ito, S.; Wehmeier, M.; Brand, J. D.; Kübel, C.; Epsch, R.; Rabe, J. P.; Müllen, K. *Chem. Eur. J.* **2000**, *6*, 4327–4342. Iyer, V. S.; Wehmeier, M.; Brand, J. D.; Keegstra, M. A.; Müllen, K. *Angew. Chem., Int. Ed. Engl.* **1997**, *36*, 1604–1607. Simpson, C. D.; Brand, J. D.; Berresheim, A. J.; Przybilla, L.; Räder, H. J.; Müllen, K. *Chem. Eur. J.* **2002**, *8*, 1424–1429. Watson, M. D.; Fechtenkötter, A.; Müllen, K. *Chem. Rev.* **2001**, *101*, 1267–1300.
- Kübel, C.; Eckhardt, K.; Enkelmann, V.; Wegner, G.; Müllen, K. *J. Mater. Chem.* **2000**, *10*, 879–886.
- Simpson, C. D.; Matternsteig, G.; Martin, K.; Gherghel, L.; Bauer, R. E.; Räder, H. J.; Müllen, K. *J. Am. Chem. Soc.* **2004**, *126*, 3139–3147.
- Deichmann, M.; Näther, C.; Herges, R. *Org. Lett.* **2003**, *5*, 1269–1271.
- Naarmann, H.; Hanack, M.; Mattmer, R. *Synthesis* **1994**, 477–478.
- Kovacic, P.; Jones, M. B. *Chem. Rev.* **1987**, *87*, 357–379.
- Three other intermediates were claimed in the patent literature, but characterization was not provided (Halleux, A. L. US 3000984, 1961).
- Lessene, G.; Feldman, K. S. In *Modern Arene Chemistry: Concepts, Synthesis, and Applications*; Astruc, D., Ed.; John Wiley & Sons: New York, 2002; pp 479–538.
- Tanaka, M.; Nakashima, H.; Fujiwara, M.; Ando, H.; Souma, Y. *J. Org. Chem.* **1996**, *61*, 788–792.
- Balaban, A. T.; Nenitzescu, C. D. In *Friedel–Crafts and Related Reactions*; Olah, G. A., Ed.; Wiley & Sons: New York, 1964; Vol. 2, part 2, pp 979–1047.
- Calculations were performed at the B3LYP 6-31G(d) level, *E*, ZPE, G_{298} from frequency calculations and ($\Delta G_{\text{sol}}(\text{CH}_2\text{Cl}_2)$) from single-point solvation calculations; see the Supporting Information for full details.
- Kryachko, E. S.; Nguyen, M. T. *J. Phys. Chem. A* **2001**, *105*, 153–155.
- Cristiano, M. L. S.; Gago, D. J. P.; Gonsalves, A. M. d' A. R.; Johnstone, R. A. W.; McCarron, M.; Varejão, J. M. T. B. *Org. Biomol. Chem.* **2003**, *1*, 565–574.
- Dewar, M. J. S.; Goodman, D. W. *J. Chem. Soc., Faraday Trans. 2* **1972**, *68*, 1784–1788.
- Staroverov, V. N.; Scuseria, G. E.; Tao, J.; Perdew, J. P. *J. Chem. Phys.* **2003**, *119*, 12129–12137.
- Curtin, D. Y. *Rec. Chem. Prog.* **1954**, *15*, 111–128.
- Randić, M.; Guo, X. *New J. Chem.* **1999**, *23*, 251–260.
- Hammond, G. S. *J. Am. Chem. Soc.* **1955**, *77*, 334–338.
- Thomaides, J.; Maslak, P.; Breslow, R. *J. Am. Chem. Soc.* **1988**, *110*, 3970–3979.

JA04613D